MICRO-DOPPLER BASED CLASSIFYING FEATURES FOR AUTOMOTIVE RADAR VRU TARGET CLASSIFICATION

Honghui Yan
Wolfgang Doerr
Alexander Ioffe
Henrik Clasen

Advanced Engineering, Delphi Deutschland GmbH
Germany

Email: {Honghui.Yan, Wolfgang.Doerr, Alexander.Ioffe, Henrik.Clasen}@delphi.com

Paper Number: 17- 0238

ABSTRACT

In order to increase traffic safety, automotive radar based Vulnerable Road User (VRU) detection and classification approaches are drawing more and more attention in recent years. There has been a growing interest in the potential use of micro-Doppler features in discrimination of VRU targets, e.g. pedestrians and cyclists.

In the paper, micro-Doppler of pedestrians and cyclists is examined by using actual data from Delphi 76GHz radar sensors as well as by computer simulations. Some practical issues in actual automotive radars, such as transmission gaps, thresholding, as well as the effect of target speed on micro-Doppler generation are discussed in the paper.

In addition, in order to apply micro-Doppler into VRU classification, the micro-Doppler pattern could be decomposed, and parameters could be estimated afterwards. In the paper, micro-Doppler decomposition and parameter estimation is discussed based on a SVD (Singular Value Decomposition) method. One of the SVD matrixes contains time dependent information, where the period/cycle of micro-Doppler pattern can be estimated. Another matrix contains information e.g. micro-Doppler spreads, symmetry, where relationship between different motion parts of the targets can be discovered.

1. INTRODUNCTION

Automotive radars are widely used in various applications [1][2], e.g. Advanced Emergency Braking (AEB) and adaptive cruise control (ACC), as well as autonomous driving. The discrimination and classification of Vulnerable Road Users (VRU), such as pedestrians and cyclists, are more and more important for those applications, and drawing attention of automotive industry.

In recent years classification of VRU targets has been widely investigated, suggesting that micro-Doppler signatures are promising for target discrimination [3][4]. It is well known that the relative movement between the radar and targets induces the Doppler effect. The relative movement here generally means main body (i.e. pedestrian torso, bike frame) motion with respect to the radar. Beside the main body motion, there exist relative motions between the radar and target components, such as periodic swinging of the legs/arms, the rotation of the wheels/pedals of the bike for VRU targets. The Doppler effect induced by those relative motions between the radar and target components is usually named Micro-Doppler in literature [3].

The micro-Doppler signature of the target is a superposition of Doppler shifts from each individual component. If a component of the target has a distinct rotation or translation, this part will return unique Doppler causing a spread in the Doppler spectrum. The spectrum width indicates the maximum velocity of the micro-motions relative to the main velocity component. In addition, many VRU micro-motions are of periodic nature, i.e., the swinging of arms/legs and the rotation of wheels. The corresponding spectrograms are periodic as well.

The micro-Doppler feature of targets is characteristic for different target classes. Pedestrians, animals, cyclists, cars have different micro-Doppler signatures. In lots of studies, micro-Doppler signature is exploited to discriminate those objects to enhance driving safety.

This paper discusses the characteristics of VRU micro-Doppler in automotive application scenarios. Practical issues which should be taken into consideration for actual automotive radars are discussed.

2. MICRO-DOPPLER CHARACTERISTICS OF VRU TARGETS

The micro-Doppler of VRU targets typically comprises a number of pattern cycles due to the periodic motion of the targets. Those pattern cycles are constructed by a couple of frequency components which correspond to different motion parts of the target. The pattern cycles and the characteristic of the frequency components are important features for target classification. Taking pedestrian as an example, VRU micro-Doppler pattern is discussed in this section.
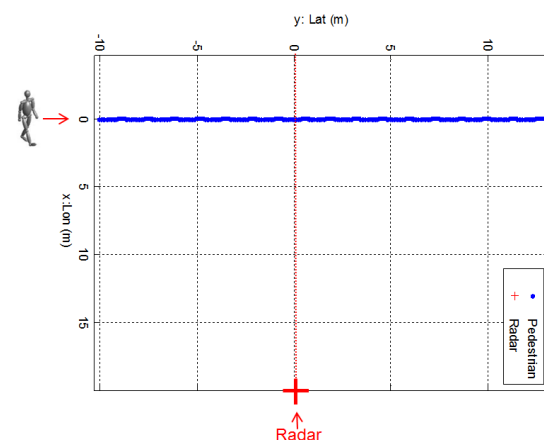
2.1 MICRO-DOPPLER OF PEDESTRIANS

Figure 1~Figure 3 show some pedestrian micro-Doppler spectrograms. There are generated via computer simulation for the scenarios: laterally moving pedestrian, longitudinally approaching pedestrian, and 45° approaching pedestrian scenarios, respectively. In the simulation, a kinematic human model is used [3][5].
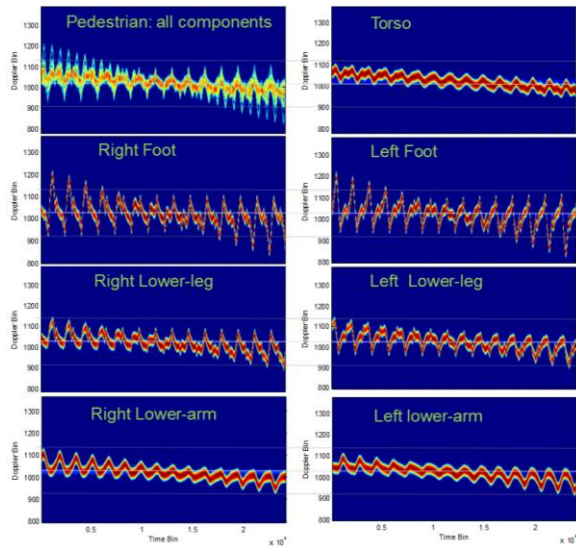
Radar parameters in the simulation:
- Radar frequency: 76.5GHz;
- Range resolution: 0.4m.
- Radar height over the ground: 0.6m;

Pedestrian parameters in the simulation:
- Pedestrian relative speed: 1m/s;
- Pedestrian height: 1.8m

(a) Laterally moving pedestrian scenario. Blue line: pedestrian moving track; red line: radar boresight

H.Yan, W.Doerr, A.Ioffe, H.Clasen

(b) Micro-Doppler pattern

Figure 1. Laterally moving pedestrian. The horizontal line @ Doppler-bin=1024 is the position of zero-Doppler.

As seen in the figures, the pedestrian micro-Doppler is constructed by the contributions from each individual body component, i.e. torso, arm, foot, etc. It can be observed that

- **Micro-Doppler magnitude and spectrum width**: the micro-Doppler of feet has the largest magnitude variation due to the fact that feet have the largest relative speed as compared with other body components. Consequently, the feet have the largest spectrum width. Similarly, lower-leg and low-arm have a larger micro-Doppler magnitude and spectrum width as well, compared with that of the torso.

  In addition, it is noted that micro-Doppler magnitude and spectrum width are illumination geometry dependent. For example, it is with a small value in the centre of Figure 2 (b) and in the right side of Figure 3 (b), where relative speeds are small due to the illumination geometries described in Figure 2 (a) and Figure 3 (a). The micro-Doppler magnitude and spectrum width for each individual body component are constant for the longitudinally moving pedestrian scenarios for the fact that illumination geometry does not vary during the data collection period.

- **Strength/energy of the pattern**: the torso component is the strongest, while that of feet is much weaker. A certain strength level is required to ensure a robust detection and classification.

- **Spectrum symmetry**: spectrum symmetry differs for different scenarios. In global micro-Doppler spectrogram sense, micro-Doppler spectrum is symmetric over gait cycles for longitudinally moving pedestrians; and symmetric with respect to the intersection of the zero-Doppler line and the radar bore-sight for laterally moving pedestrians. However, the spectrum is asymmetric for 45° moving pedestrians since that the spectrum magnitude decreases when targets approach the radar.

- **Pattern Cycle**: pattern cycle is gait cycle dependent. Typically the duration of the cycle is empirically around $D_{cycle} = 1.346/\sqrt{v_{tgt}}$, where v_{tgt} is the relative target speed (normalized by the thigh height) in m/s [3][4]. That is to say, the duration of the pattern cycle is pedestrian relative moving speed dependent. The faster the pedestrian, the shorter the cycle duration in micro-Doppler.
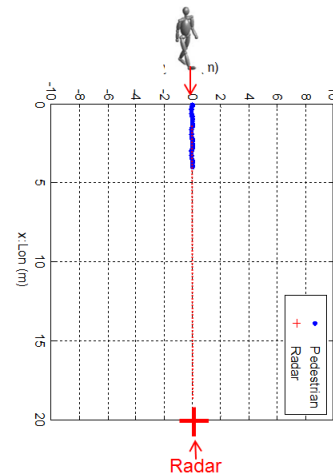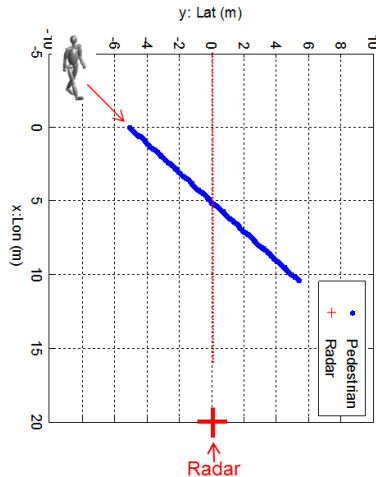

(a) Longitudinally approaching pedestrian scenario. Blue line: pedestrian moving track; red line: radar boresight
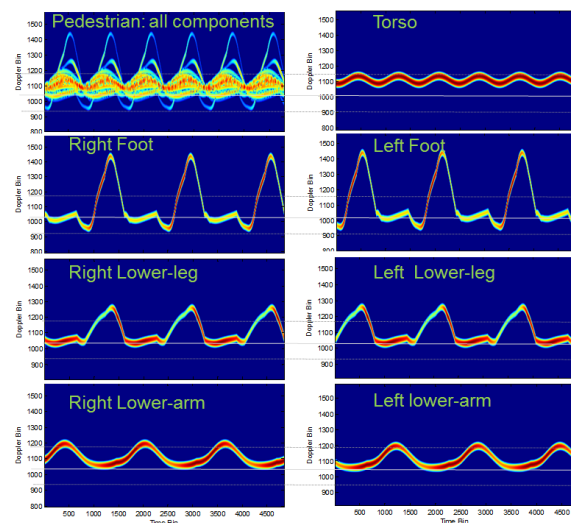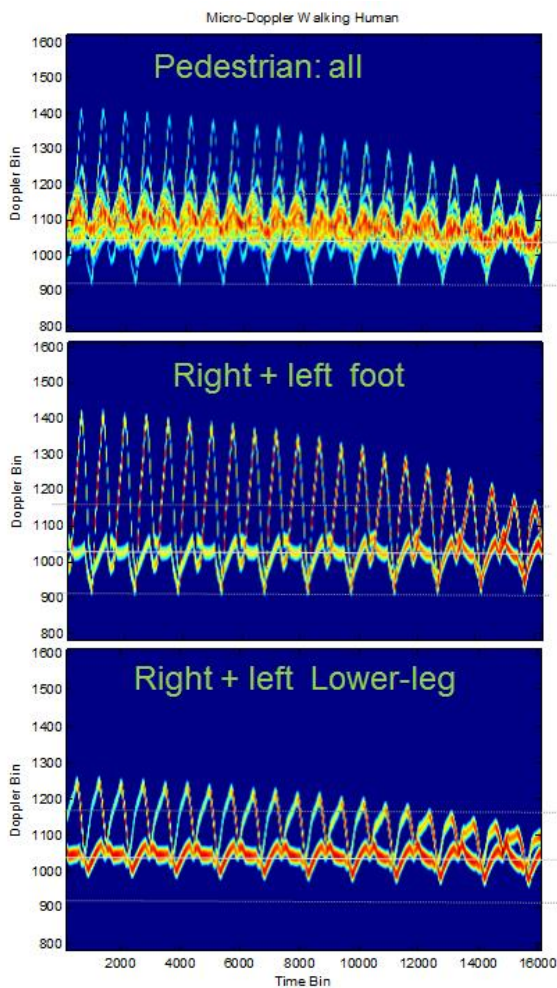

(b) Micro-Doppler pattern

Figure 2 Longitudinally moving pedestrian. The horizontal line @ Doppler-bin=1024 is the position of zero-Doppler.

(a) 45° approaching pedestrian scenario. Blue line: pedestrian track; red line: radar boresight

An actual pedestrian micro-Doppler spectrogram is given in Figure 4. It is generated by a Delphi side-looking radar. It is seen that feet, arms, and the torso have different characteristics since they have different relative motion signatures. The micro-Doppler spread of feet is much greater than others.

It is noted that the micro-Doppler of feet might be invisible under certain conditions due to weak reflection nature of the feet. As a comparison, the micro-Doppler of the body (torso) is much stronger and with good visibility. Invisibility of certain micro-Doppler components may lead classification errors.

In Figure 4, the relationship between the gait cycle and the micro-Doppler pattern is given. The gait cycle is one of the important features for pedestrian.
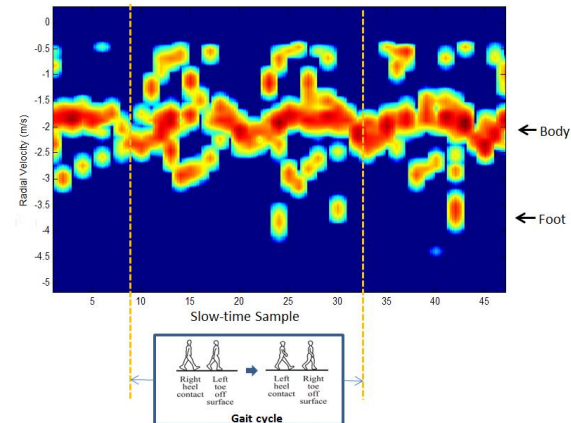

Figure 4 Pedestrian micro-Doppler pattern generated by a Delphi radar

2.2 MICRO-DOPPLER OF CYCLISTS

Figure 5 shows an actual micro-Doppler pattern acquired from a Delphi radar for a longitudinally moving cyclist. Figure 6 is the corresponding computer simulation. It is shown that cyclist micro-Doppler comprises components from, e.g. wheels, pedals/legs, as well as the bike-frame and the human-body on the bike.

For the simplification of discussion, the micro-Doppler from wheels and pedals/legs can be further split into two parts: lower part and upper part. The upper and lower parts in micro-Doppler spectrograms correspond, respectively, upper and lower part of the wheels for the concerned scenario.

(a)   Micro-Doppler pattern

Figure 3. 45° approaching pedestrian. The horizontal line @ Doppler-bin=1024 is the position of zero-Doppler.
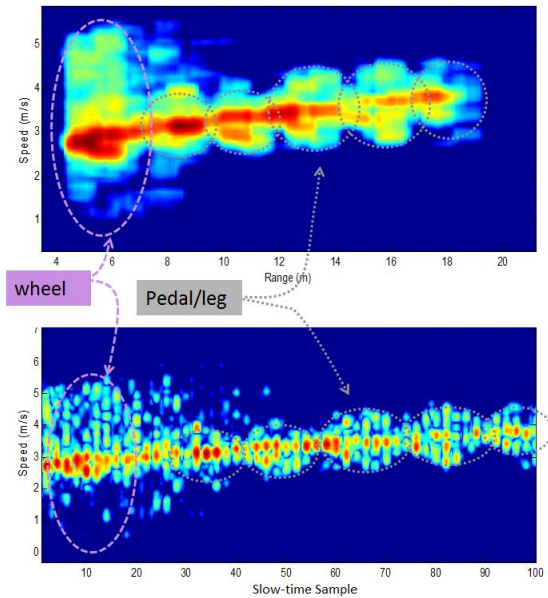
Figure 5 Longitudinally moving cyclist micro-Doppler pattern from a Delphi radar. Upper figure: micro-Doppler in speed-range domain. Lower Figure: micro-Doppler in traditional speed-slow time domain.
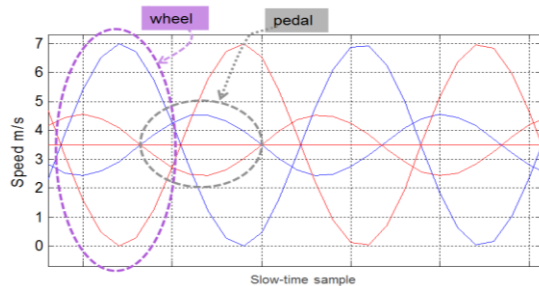

Figure 6 Simulated bike micro-Doppler (Only two reflecting points on the wheel are simulated for simplicity)

It is observed from the figures that:

- **Micro-Doppler magnitude and spectrum width**: the spectrum width of the wheels is much wider than that of pedals/legs and the bike-frame. The maximum micro-Doppler magnitude of the wheels, i.e. the upper part the wheel micro-Doppler, is approximately double that of bike-frame/axis for the concerned scenario;
- **Strength/energy of the pattern**: The lower part of the wheel micro-Doppler is much weaker than the upper part due to radar illumination geometry. However, reflection from pedals/legs is much stronger than that from wheels.

- **Spectrum symmetry**: micro-Doppler spectrum is symmetric over rotation cycles for the concerned scenario.
- **Pattern Cycle**: the pattern cycle is related to the rotation cycles of the wheels and pedals/legs, as shown in both measured and simulated patterns.

It is noted that wheel micro-Doppler might be invisible in a far range (e.g. as shown in Figure 5), due to the attenuation of the echo signal in far range as well as radar illumination geometry. It is interesting to note that pedal/leg micro-Doppler is much stronger than that of wheels. It implies that pedal/leg micro-Doppler is also a promising feature for cyclist classification.

3. SOME PRACTICAL CONSIDERATIONS IN VRU MICRO-DOPPLER EXTRACTION

3.1 EFFECT OF TRANSMISSION GAPS

In literature, there are lots of algorithms can be used for Micro-Doppler spectrogram generation e.g. Short-Time-Fourier-Transform (STFT), or Wigner-Ville distribution (WVD) based algorithms [3] etc. In those algorithms, signals to be processed are generally uniformly sampled in slow-time. That is, those algorithms cannot be directly applied for radars with non-uniform transmissions.

A popular automotive radar transmission scheme is shown in Figure 7. Usually there are gaps among transmission groups, i.e. CPI (coherent processing interval) in the figure . In signal processing point of view, the transmission can be regarded as a kind of non-uniform transmission due to the gaps. In this case, we cannot directly use the algorithms mentioned above e.g. STFT, WVD to process non-uniformly sampled data directly. An appropriate solution should be worked out for the gapped data.
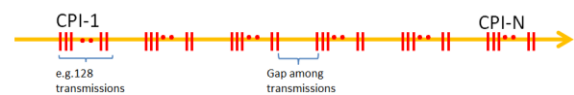

Figure 7 Example of automotive radar transmission scheme. A number of transmissions (e.g. 128) comprise a "CPI". A group of transmissions within a "CPI" is typically the basic unit for automotive radar signal processing. For instance, a range-Doppler map can be obtained by the data obtained from a certain "CPI". Transmissions within a "CPI" are typically uniformly distributed. However, sometimes there are gaps among CPIs for

actual automotive radars. In this case, transmissions are not uniform over CPIs anymore due to the gaps.

3.2 EFFECT OF THRESHOLDING

Thresholds, e.g. sensitivity, CFAR (Constant False Alarm) thresholds are widely used in automotive radar signal processing. These thresholds are used to separate objects of interest from noise and clutter, and also to limit the burden on the radar processor. It is seen in the Figure 8 that, the thresholding processing impacts greatly the performance of micro-Doppler.
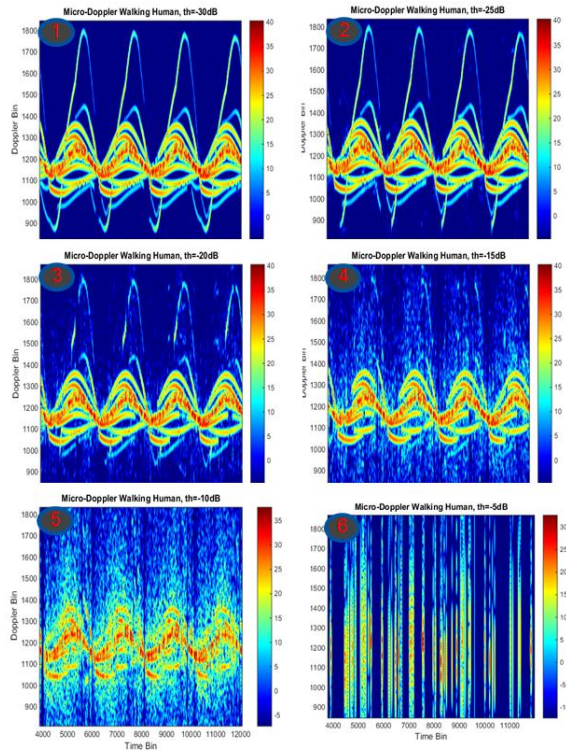

Figure 8 Effect of thresholding on micro-Doppler. Applied thresholds are -30dB, -25dB, -20dB, -15dB, -10dB, -5dB with respect to the maximum peak in the raw data domain respectively.

We apply increasing thresholds from -30dB until -5dB onto the raw-data, then apply STFT to get spectrograms as given in ①~⑥ of the Figure 8, respectively. It is seen that, the higher the threshold applied, the more details are missing in micro-Doppler. The micro-Doppler component of feet almost disappear in ④ of the figure. All the pedestrian micro-Doppler components are lost in ⑥ of the figure when a high threshold is applied. It implies that, in order to get effective micro-Doppler features, the radar must have the sensitivity

to extract these features from the noise floor of the sensor and from the surrounding clutter; and the threshold levels should be appropriately set in data preparation.

3.3 EFFECT OF VRU TARGET SPEED ON MICRO-DOPPLER EXTRACTION

The relative target speed is usually involved in the determination of Pulse Repetition Frequency (PRF), as well as in the estimation of the number of scans which are needed for pattern classification and recognition.
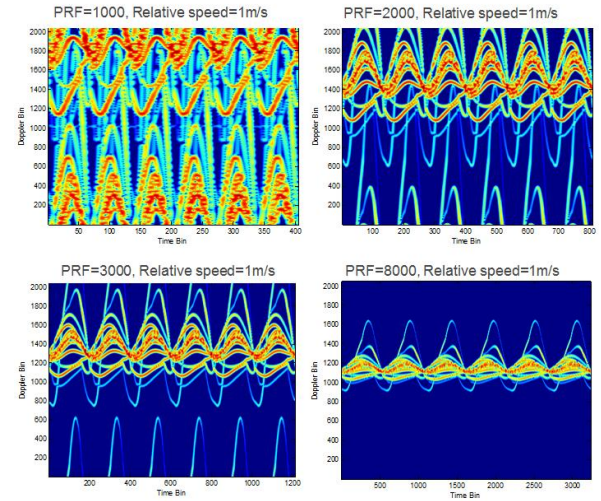

Figure 9 Relative speed and PRF. Radar Frequency: 77GHz. Here relative speed is the relative speed between human torso and the radar. It is not the maximum relative speed between the body components and the radar.

Taking the scenario as mentioned in Figure 2 as an example, different PRF rates, i.e. PRF=1000, 2000, 3000, 8000 (pulse/second), are applied in the procedure of the raw data generation, respectively. Figure 9 shows the obtained spectrograms. As shown in the figure, micro-Doppler pattern will be ambiguous if PRF is too low. In order to get an unambiguous micro-Doppler pattern, PRF should be appropriately set. Generally for FMCW radar system, PRF can be set as

$$PRF \geq 4v_{max}/\lambda$$

where λ is the wavelength, and v_{max} is the maximum relative speed between the radar and the target components. Actually $2v_{max}/\lambda$ is the maximum Doppler frequency induced by motion of target components. That is PRF should be

greater than twice of the maximum Doppler frequency.

It is noted that, v_{max} is not the relative speed between the human body (i.e. torso) and the radar. Usually, it is the relative speed between feet and the radar. The relative speed of feet could be much higher than that of body/torso. For most moving pedestrians, the PRF can be set e.g. >11k for stationary millimeter automotive radars. An even higher PRF, e.g. 35K, can be selected for the case of moving radar host vehicles (e.g. with speed of < 70km/h) with targets e.g. typical pedestrians and cyclists.

In order to recognize/classify VRU targets, a certain number of micro-Doppler pattern cycles need to be collected. Generally, the more micro-Doppler pattern cycles are available, the higher the classification performance. In the generation of micro-Doppler pattern a number of scans are required by the micro-Doppler processor for each micro-Doppler cycle. Taking pedestrian micro-Doppler as an example, Figure 10 shows the relationship between the target speed and the number of scans required by a micro-Doppler cycle. The slower the target, the more scans (in other words, the more time) are needed to obtain one micro-Doppler cycle.

Let's consider the case that the radar approaches the target with a high speed, and the case that the radar locates in a close range to the target. In both case, the available observation time is very short due to the high relative speed, and a closer range. The shorter the observation time, the less possibility the targets are correctly classified. Extremely, the available observation time cannot support generation of a full micro-Doppler cycle. In this case, VRU classification would become even more challenging.
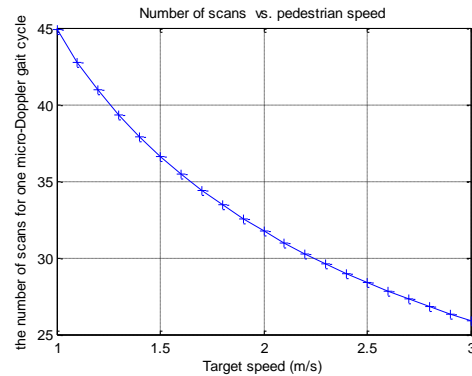

Figure 10 Number of scans vs. pedestrian speed for a micro-Doppler gait cycle, @ scan-period=30ms. It is noted that the x-axis is target speed over ground. It is not the relative speed with respect to the radar.

4. MICRO-DOPPLER DECOMPOSITION AND PARAMETER ESTIMATION

The micro-Doppler patterns e.g. as shown in Figure 1~Figure 5, usually cannot directly be used for target classification. Typically classifying features should be extracted based on those patterns. One of the possible micro-Doppler feature extraction approaches is to decompose the micro-Doppler pattern by e.g. Singular Value Decomposition (SVD) based solutions [6][7].

Figure 11 gives an example of micro-Doppler decomposition. Using the data as shown in Figure 2(b), labeled with "Pedestrian, all components", the micro-Doppler pattern can be decomposed into three matrixes U, S, V, by using SVD approach as shown in Figure 11, where

- The matrix U contains time dependent information. The period/cycle of micro-Doppler pattern can be estimated from this matrix.
- The matrix S contains amplitude information.
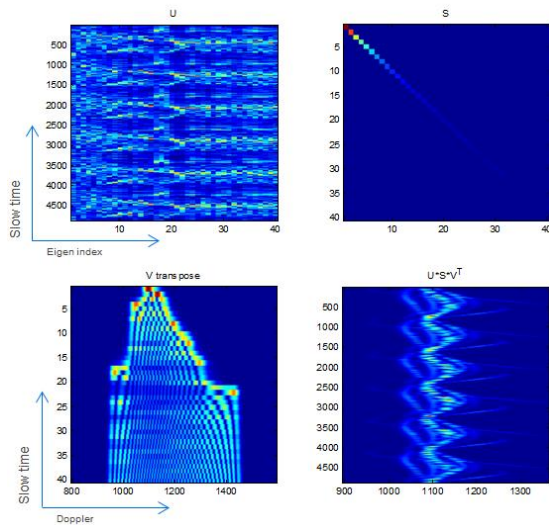- The matrix V contains Doppler information Doppler spread, and symmetry can be estimated

Figure 11 Micro-Doppler decomposition for the data as shown in Figure 2(b), labeled with "Pedestrian, all components".
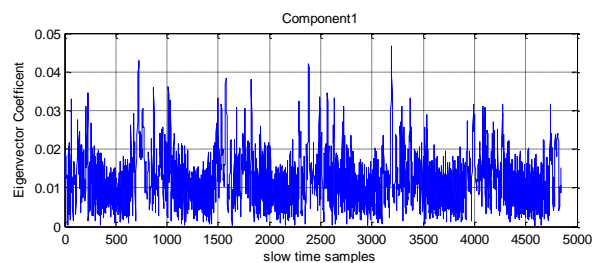

Figure 12 One of the components in matrix U.

The advantage of above approach is that micro-Doppler feature is not affected by RCS/amplitude of the signal, since the matrix U and V are RCS/amplitude independent.

Figure 12 shows one of the components in matrix U. As an example of parameter estimation based on decomposed matrixes, parameters e.g. pattern cycles can be estimated from Figure 12.

5. CONCLUSIONS

In order to explore the VRU micro-Doppler signatures, the characteristic of micro-Doppler is investigated under different scenarios by simulation and radar measurement.

As expected, for pedestrians the feet have the largest micro-Doppler spread as compared with other body components. However, it not always visible in an actual automotive radar measurement

due to the weak reflection and illumination geometry for some cases. Micro-Doppler pattern differs scenarios, e.g. longitudinally -, laterally-, or 45° moving scenarios.

For cyclists, both of the wheel and pedal have circular shape micro-Doppler patterns. However, the reflection from pedals is much stronger than that of wheels. Both of the wheel and pedal micro-Doppler are important features for cyclist classification.

REFERENCES

[1]. A. Ioffe, W. Doerr, H. Yan, D. H. Vu and A. H. Arage, "RCS characteristics of street curbs and the applications in automotive radar classification," 2016 European Radar Conference (EuRAD), London, United Kingdom, 2016, pp. 241-244.

[2]. R. Khlifi, M. Wurth, A. Ioffe, U. Iurgel, W. Doerr, "360° Radar based parking", IQPC International Conference "The Road to Automated Drive 2014" and "Chassis Sensors & 360° Sensing", Stuttgart, Germany, 2014

[3]. V.C. Chen, "The Micro-Doppler Effect in Radar", Artech House, 2011

[4]. B.Rodriguez-Hervas, M.Maile, B.C. Flores, "Study of the microdoppler signature of a bicyclist for different directions of approach", Proc. SPIE 9461, Radar Sensor Technology XIX and Active and Passive Signatures VI, 94611E, May 21, 2015, doi:10.1117/12.2087619

[5]. R. Boulic, N.M.Thalmann,and D.Thalmann, "A global human walking model with real-time kinematic personification", The Visual Computer, 1990, vol6 pp344~358

[6]. C. Clemente, A.W. Miller, J.J.Soraghan, "Robust principal component analysis for micro-doppler based automatic target recognition", 3rd IMA conference on Mathematics in Defence, 2013, Malvern, United Kingdom

[7]. J. J. M. de Wit, R. I. A. Harmanny and P. Molchanov, "Radar micro-Doppler feature extraction using the Singular Value Decomposition," 2014 International Radar Conference, Lille, 2014, pp. 1-6.